

AD-A088 423

CORNELL UNIV ITHACA NY DEPT OF CHEMISTRY
A STUDY OF SECONDARY ION TRIPLE BOND ANALOGUES. (U)
AUG 80 D T HODUL, W C HARRIS, G H MORRISON

F/G 20/12

N00014-80-C-0538

UNCLASSIFIED

TR-1

MI

[OF]

AD-A088423



END
DATE
FILMED
9-80
DTIC

LEVEL

54

(12)

OFFICE OF NAVAL RESEARCH

Contract N00014-80-C-0538

Task No. NR 051-736

TECHNICAL REPORT NO. 1

AD A088423

A Study of Secondary Ion Triple Bond Analogues
by

D.T. Hodul, W.C. Harris, and G.H. Morrison

Prepared for publication

in the

International Journal for Mass Spectrometry and Ion Physics

Cornell University

Department of Chemistry

Ithaca, N. Y. 14853

August 20, 1980

DTIC
ELECTE
AUG 26 1980
S C D

Reproduction in whole or in part is permitted for
any purpose of the United States Government

This document has been approved for public release
and sale; its distribution is unlimited

DDC FILE COPY

80 8 25 004

REPORT DOCUMENTATION PAGE		READ INSTRUCTIONS BEFORE COMPLETING FORM
1. REPORT NUMBER Technical Report No. 1	2. GOVT ACCESSION NO. AD-A088423	3. RECIPIENT'S CATALOG NUMBER
4. TITLE (and Subtitle) A STUDY OF SECONDARY ION TRIPLE BOND ANALOGUES		5. TYPE OF REPORT & PERIOD COVERED Interim Technical Report
7. AUTHOR(s) D.T. Hodul, W.C. Harris, G.H. Morrison		8. CONTRACT OR GRANT NUMBER(s) N00014-80-C-0538
9. PERFORMING ORGANIZATION NAME AND ADDRESS Department of Chemistry Cornell University Ithaca, N. Y. 14853		10. PROGRAM ELEMENT, PROJECT, TASK AREA & WORK UNIT NUMBERS NR-051-736
11. CONTROLLING OFFICE NAME AND ADDRESS ONR (472) 800 North Quincy St. Arlington, Va. 22217		12. REPORT DATE August 20, 1980
14. MONITORING AGENCY NAME & ADDRESS (if different from Controlling Office) 14) TR-2		13. NUMBER OF PAGES 18 pages
		15. SECURITY CLASS. (of this report) Unclassified
		15a. DECLASSIFICATION/DOWNGRADING SCHEDULE
16. DISTRIBUTION STATEMENT (of this Report) Approved for public release: distribution unlimited		
17. DISTRIBUTION STATEMENT (of the abstract entered in Block 20, if different from Report)		
18. SUPPLEMENTARY NOTES Prepared for publication in International Journal of Mass Spectrometry and Ion Physics		
19. KEY WORDS (Continue on reverse side if necessary and identify by block number) Secondary Ion Mass Spectrometry, molecular ions, semiconductors, ion implantation		
20. ABSTRACT (Continue on reverse side if necessary and identify by block number) Diatomic molecular ions isoelectronic with CN ⁻ have been generated in ion implanted semiconductor materials and analyzed using secondary ion mass spectrometry (SIMS). Negative (IVA-VA) ⁻ ions containing the VA species from IVA implanted IIIA-VA semiconductors are found to be produced more readily than the IVA ⁻ ions. The triple bond analogues studied were of the general type (IVA-VA) ⁻ , (IIIA-VIA) ⁻ , (VA-VIA) ⁻ & (IVA-VIIA) ⁻ . Molecular ion formation mechanisms and the analytical consequences of the results of this study are discussed.		

AD-A088423

A STUDY OF SECONDARY ION TRIPLE BOND ANALOGUES*

D. T. Hodul**, W. C. Harris and G. E. Morrison***

Department of Chemistry
Cornell University
Ithaca, N.Y. 14853

ABSTRACT

Diatomic molecular ions isoelectronic with CN^- have been generated in ion implanted semiconductor materials and analyzed using secondary ion mass spectrometry (SIMS). Negative (IVA-VA) $^-$ ions containing the VA species from IVA implanted IIIA-VA semiconductors are found to be produced more readily than the IVA $^-$ ions. The triple bond analogues studied were of the general type (IVA-VA) $^-$, (IIIA-VIA) $^-$, (VA-VIA) $^+$ and (IVA-VIIA) $^+$. Molecular ion formation mechanisms and the analytical consequences of the results of this study are discussed.

*This work was supported by the National Science Foundation, the Office of Naval Research, and the Cornell Materials Science Center.

**Present address: Chemistry Division, Argonne National Laboratory, Argonne, Illinois, 60439.

***Author to whom reprint requests should be addressed.

Accession for	<input checked="" type="checkbox"/>	<input type="checkbox"/>	<input type="checkbox"/>
NIL	GA&I		
DS	TAE		
Unannounced			
Justification			
By			
Classification			
Approved for Release			
Authority			
Dist. Statement			
Dist. Statement			
A			

INTRODUCTION

Secondary molecular ions have been observed as sputtering products in a wide variety of materials and over a large range of experimental conditions [1-12]. Many mechanisms of secondary ion formation have been proposed [13-21], but a complete picture has not yet emerged [22,23]. Several modeling approaches to molecular ion emission have been taken [24-30], but evidence from computer simulations of sputtering [27,31-34] indicates that molecular ion formation is generally due to atomic recombination. Additional basic studies into the formation of cluster ions have measured secondary energy spectra [35-42] and the effects of surface adsorbed gases on secondary yields [43,44]. A major motivation for understanding molecular ion processes derives from analytical applications in surface analysis. For example, molecular ions have been used to improve sensitivity and detectability of impurities through production of high yield molecular ions [45-47] and energy discrimination methods [42,48]. SIMS can also be used to produce unusual molecular species for study of both surface [49] and molecular chemistry [45,50,51].

In this paper we describe a study of secondary molecular ions isoelectronic with CN^- , i.e. triple bond analogues. Silicon, germanium and several III-V semiconductors have been implanted with IIIA-VIIA elements. The mass analyzed secondary ion signals of the implant ("impurity") I^\pm and matrix/implant MI^\pm molecular species have been measured. Mechanisms of molecular ions are discussed as they pertain to our results, and general and specific analytical implications are noted. Finally, a procedure for predicting high signal molecular secondary ions is outlined, and the additional studies to be derived from our results are listed.

EXPERIMENTAL

The choice of triple bond analogue ions for this study was based on several considerations. When analyzing semiconductor and solar cell materials for group IIIA impurities using an oxygen beam, the negative secondary mass spectrum always contained III-O⁻ levels that were 10-100 times larger than the IIIA⁻ level. Exploratory experiments of phosphorous implanted silicon showed large SiP⁻ as well as SiC⁻ levels, the carbon impurity originating from vacuum contamination even at a vacuum of $< 10^{-5}$ pascal [52]. We felt these high molecular ion yields were due to the strong bonding in these species, and tested this hypothesis on a wide variety of isoelectronic ions. These species proved particularly appropriate, as selection of the desired implant impurity in a semiconducting matrix allowed construction a large number of secondary molecular ions as well as ease of analysis. The important advantage of implantation to introduce "impurities" is the characteristic gaussian concentration profile which results. Mass analyzed secondary ions can be demonstrated to contain the implanted species when this depth profile is seen. This known concentration profile also provides a means of correcting mass interferences and for ratioing yields [53]. For this study IIIA-VIIA elements were implanted in Si, Ge, GaAs, InP, InSb, and GaP. A description of the implantation procedures and fluences is given in reference 46.

The SIMS analysis was performed using a CAMECA IMS-300 ion microanalyzer which has been previously described [54]. A 200- μm contrast aperture was used and the electrostatic sector tuned for maximum sensitivity. The primary ion conditions used were O₂⁺/O⁺ beam of 1.0 μA . Oxygen was chosen to enhance secondary yields [55,56]. For positive secondary ion detection a 5.5-keV primary beam was rastered over a 700 x 700 μm^2 area at a 33° incidence; for

negative secondaries a 14.5-keV beam over $580 \times 580 \mu\text{m}^2$ at 57° incidence was used. In both cases secondaries were detected normal to the surface. Table 1 lists the possible combinations of implant and matrix that can result in triple bond secondary ions. Several analyses with obvious mass interferences were not performed, e.g. AlS^- due to the interference of AlO_2^- . These cases as well are indicated in Table 1.

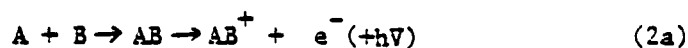
The signal of the implant ion I^\pm and the matrix/impurity molecular ion MI^\pm were monitored simultaneously as a function of sputtering time. Profiles were taken well past the implant depth to determine background interferences. These interferences were subtracted from the total signal obtained before $\text{MI}^\pm/\text{I}^\pm$ ratios were calculated. The signals at the implant maxima were ratioed.

RESULTS AND DISCUSSION

While there is considerable debate on the exact processes occurring during ion bombardment of a surface, over the last several years a consensus has formed on several aspects of the process. These need to be included in any model of ion sputtering. An individual primary ion collides with the sample surface and produces a cascade of momentum transfers between the atoms of the solid. This collision cascade is well described by classical mechanics and has characteristic dimensions of $\sim 100 \text{ \AA}$ and $10^{-13} - 10^{-14}$ sec. Secondary neutrals and ions are ejected as a result of this momentum transfer in three time scales: 1) short, i.e. 10^{-14} sec, as a result of momentum transfer during the initial impact, 2) intermediate, i.e. 10^{-13} sec, as a result of many collisions in the cascade, 3) thermal processes, i.e. $> 10^{-13}$ sec, as a result of heating of the surface as the cascade relaxes.

Secondary ions are produced in both ion thermal events; however, the ionization mechanisms are not well understood. Regardless, the ionization yield (number of secondary ions per primary ion) is known to depend exponentially on the ionization potential of the secondary species (or the electron affinity for negative secondaries), and any model of the ionization process must reflect this behavior [23].

Although secondary molecule and molecular ion formation has also been studied and mechanisms postulated, here too a generalized approach has not been developed. Questions about cluster formation mechanisms partly derive from a lack of understanding of the sputtering process itself, but more importantly we feel molecular ion formation is strongly matrix dependent, necessitating models which incorporate specific experimental and instrumental details. One can envision two processes which lead to sputtered clusters; 1) the molecule is ejected intact as it existed on the surface, or 2) recombination is ejected atomic species very near the surface. For molecular ions to form in the first case ionization mechanisms would be analogous to that of atomic secondary ions, and molecular ion yields would depend on both the molecular ionization potential (electron affinity) and the bond energy. The recombination mechanisms, however, might proceed through several processes, for example:



Many other processes might be imagined. It is possible, however, to divide all the recombination mechanisms into those where the reactant atoms are ionized before recombination (as in reaction 1.), and those where ionization occurs after the recombination, possible through an excited intermediate (as in reaction 2.). Reactions of the first type can reasonably produce either positive or negative secondary molecular ions; the yield of AB^{\pm} will depend on the ion to neutral yield ratios and atomic concentrations of A and B, as well as the stability of the AB^{\pm} species. For reactions of the second type the ionization processes will be different for positive and negative clusters. For positives the reaction will likely proceed through an excited state (or transition state as defined by the lifetime of the intermediate) with an electron being ejected to produce the final ionized state. Negative ionization, however, is less probable as it requires capture of an electron from the surface. Such recombination is likely to occur too far from the surface for electron capture by the molecule. Therefore, mechanisms similar to 2b for negative cluster formation should be rejected in favor of those represented by reaction 1.

Additionally, there are some specific concerns regarding the use of ion implantation and the interpretation of our results. We assume that ion implantation of these semiconductors has produced a homogeneous random distribution of impurity species, and there is no precipitate formation even to an atomic scale. Further, as gaussian profiles are observed, we assume the impurity concentration does not affect the ionization yield in the material, i.e. impurity signals vary linearly with concentration.

Results of the experiment are given in Table 1. Specific difficulties for individual samples are given in footnotes to this table. A selected depth

profile run is shown in Figure 1 for phosphorous implanted germanium. High initial signals result from enhanced ionization caused by surface oxides which are quickly sputtered away. Results of the depth profile of antimony implanted in silicon are given in Figure 2. The SiSb^- profile is the typical gaussian seen for implanted species or molecular ions containing the implanted atom. However, the Sb^- signal shows unusual behavior due to mass interferences of $m/e = 121$ of $^{28}\text{Si}^{29}\text{SiO}_4^-$ and $^{28}\text{SiO}_4\text{H}^-$. Similar anomolous behavior has been observed in other SIMS analysers of implanted silicon. This can be rationalized as crystal damage caused by implantation (e.g. references 57,58) which is particularly important for implanted silicon (e.g. 57,60).

Several trends can be seen in these data. These trends are of two types, those resulting from bonding considerations of the secondary ion and those resulting from the mechanics of the sputtering process. Two trends of the bonding type are evident from the data. First, negative secondary molecular species are more stable than positive species. Out of 18 possible MI^+ molecules possible from our experimental design only AsTe^+ showed an appreciable MI^+ to I^+ yield ratio and many of these positive triple bond analogues were not seen at all. Not shown in Table 1 are molecules containing oxygen from the primary beam, i.e. $(\text{IVA-O})^+$ species. Molecules of this type showed moderate OI^+ to I^+ yield ratios close to unity. However, this does not significantly affect agruement about the greater stability of negative clusters. This can be seen when the positive and negative yield ratios for oxygen beam/impurity species are compared. That is for molecules of the type $(\text{IIIA-O})^-$ generally $(\text{IIIA-O})^- / (\text{IIIA}^-) \approx 10$.

Second, MI^{\pm}/I^{\pm} tends to be largest when M and I are of similar molecular weight. This is a result of the stronger bonding expected from the close match in the energies of the bonding electrons for atoms in the same period. A notable exception is the beam/impurity species InO^- , where $InO^-/In^- \approx 10$ for indium implanted in Ge and indium implanted in gallium arsenide.

While the bonding of the secondary ion clearly plays an important role in understanding molecular ion yields, the details of the sputtering event must be included in a more complete description. A clear trend can be seen in the ratio of ion yields. Molecular ions which contain a matrix atom of high atomic ion yield also are produced in high yields. This is expected if the molecular ion is formed as described in Equation 1. For example, look at the system of highest MI^-/I^- , germanium implanted in indium phosphide analyzed for GeP^- . By Equation 1 the following mechanisms are proposed:



An expression similar to expressions of rate equations for reactions in the gas phase can be written:

$$[GeP^-] = k_1[Ge][P^-] + k_2[Ge^-][P] \quad (5)$$

where [] indicates yields per cascade and k_1 and k_2 are constants which depend on the details of the cascade, i.e. primary beam energy, angle and mass, the bond energy of GeP^- , and the frequency of molecular formation per collision. Equations 3, 4 and 5 are also valid for the sample phosphorous implanted in germanium analyzed for GeP^- , but the yield ratio GeP^-/P^- is about four times smaller than GeP^-/Ge^- for germanium implanted in indium phosphide. If k_1 and k_2 are approximately the same, this implies $[P^-]/[Ge^-] \approx 4$, in qualitative

agreement with arguments based on electron affinities. Therefore dominant recombination to form GeP^- is given by Equation 3, and supports the rejection of post recombination ionization mechanism for negative molecular ions.

These observations and some interesting analytical consequences and led to several predictions on how to analyze low yield impurity species. In cases where M^+/I^+ is greater than one, I^+ is best analyzed using MI^+ . More interesting is the possibility of selecting the primary beam species to produce high sensitivity molecular ions when no matrix/impurity molecular is produced. For example, if a negative secondary mass analysis is desired, where Ge^- is an impurity to be analyzed, a P^+ primary beam could be used to produce the higher sensitivity GeP^- species. Schemes to remove mass interferences, but maintain high sensitivity can also be imagined.

We have demonstrated that studies of molecular ion formation using ion implantation can yield a wide variety of information about the sputtering process. This knowledge can then be used to solve specific analytical problems, and also suggests several additional studies: 1) analyses of larger cluster species, 2) studies of transition metal implants, 3) energy spectra determinations to test molecular formation models, and 4) double implant experiments to monitor the molecular formation of the implant/implant molecular ion species.

REFERENCES

1. M. Leleyter and P. Joyes, LeJournal de Physique, C2 (1977) 11.
2. G. Hortig and M. Muller, Zeitschrift für Physik, 221 (1969) 119.
3. G. Staudenmaier, Rad. Eff., 13 (1972) 89.
4. R.F.K. Herzog, W.P. Poschenrieder, and F.G. Satkiewicz, Rad. Eff., 18 (1973) 199.
5. M. Leleyter and P. Joyes, Rad. Eff., 18 (1973) 105.
6. M. Leleyter and P. Joyes, J. Phys. B, 7 (1974) 516.
7. A. Shepard et al., Chem. Phys. Lett., 44 (1976) 371.
8. J.A. Taylor and J.W. Rabalais, Surf. Sci., 74 (1978) 229.
9. F. Honda, G. Lancaster, and J. Rabalais, Surf. Sci., 76 (1978) L613
10. F.M. Devienne, M. Teisseire, and R. Combarieu, Comptes Rendus des Seances de l'academie des Sciences, Series C, 288 (1979) 1.
11. G. Lancaster, F. Honda, Y. Fukuda, and J. Rabalais, Int. J. Mass Spec. and Ion Phys., 29 (1979) 199.
12. F. Honda, Y. Fukuda, and J.W. Rabalais, J. Chem. Phys., 70 (1979) 4834.
13. P. Sigmund, Phys. Rev., 184 (1969) 383.
14. C.A. Andersen and J.R. Hinthorne, Anal. Chem., 45 (1973) 1421.
15. P. Joyes, Rad. Eff., 19 (1973) 235.
16. J.M. Schroer, T.N. Rhodin, and R.C. Bradley, Surf. Sci., 34 (1973) 571.
17. Z. Svroubek, Surf. Sci., 44 (1974) 47.
18. M. Cini, Surf. Sci., 54 (1976) 71.
19. F.G. Rüdenauer, W. Steiger, and H.W. Werner, Surf. Sci., 54 (1976) 553.
20. H.G. Prival, Surf. Sci., 76 (1978) 443.
21. K.R. Pollitt, J.C. Robb, and D.W. Thomas, Nature (London), 272 (1978) 436.
22. G. Blaise and A. Nourtier, Surf. Sci., 90 (1979) 495.
23. P. Williams, Surf. Sci., 90 (1979) 588.

24. P. Joyes, J. Phys. B, 4 (1971) L15.
25. P. Joyes, J. Phys. Chem. Solids, 32 (1971) 1269.
26. K. Wittmaak and G. Staudenmaier, Appl. Phys. Lett., 27 (1975) 318.
27. I.S. Bitenskiĭ and E.S. Parilis, Zh. Tekh. Fiz., 48 (1978) 1941.
28. F. Honda, G.M. Lancaster, Y. Fukunda, and J.W. Rabalais, J. Chem. Phys., 69 (1978) 4931.
29. A.E. Morgan and H.W. Werner, J. Chem. Phys., 68 (1978) 3900.
30. K. Wittmaack, Phys. Lett., A69 (1979) 322.
31. D.E. Harrison and C.B. Delaplain, J. Appl. Phys., 47 (1976) 2252.
32. N. Winograd, D.E. Harrison, and B.J. Garrison, Surf. Sci., 78 (1978) 467.
33. B.J. Garrison, N. Winograd, and D.E. Harrison, J. Chem. Phys., 69 (1978) 1440.
34. B.J. Garrison, N. Winograd, and D.E. Harrison, J. Vac. Sci. & Tech., 16 (1979) 789.
35. G. Staudenmaier, Rad. Eff., 18 (1973) 181.
36. G.P. Konnen, A. Tip, and A.E. deVries, Rad. Eff., 21 (1974) 259.
37. G.P. Konnen, A. Tip, and A.E. deVries, Rad. Eff., 26 (1975) 23.
38. M.A. Rudat and G.H. Morrison, Int. J. Mass Spec. and Ion Phys., 30 (1979) 197.
39. G. Blaise and G. Slodzian, Rev. Phys. Appl., 8 (1973) 105.
40. R. Laurent, G. Blaise, and G. Slodzian, Comptes Rendus des Seances l'academie des Sciences, 278 (1974) 11.
41. G. Staudenmaier, Rad. Eff., 13 (1972) 87.
42. G. Slodzian, Surf. Sci., 48 (1975) 161.
43. M. Prager, Appl. Phys., 8 (1975) 361.
44. M.A. Rudat and G.H. Morrison, Int. J. Mass Spec. and Ion Phys., 30 (1979) 233.
45. A.E. Morgan and H.W. Werner, J. Microsc. Spectrosc. Electron, 3 (1978) 495.
46. D.P. Leta and G.H. Morrison, Anal. Chem., 52 (1980) 514.
47. K. Nakamura, H. Hirose, A. Shibata, and H. Tamura, Jap. J. of Appl. Phys., 16 (1977) 1307.

48. N. Shimizu, M.P. Semet, and C.J. Allegre, Geochemica & Cosmochimica Acta, 42 (1978) 1321.
49. G.M. Lancaster, F. Honda, Y. Fukuda, and J.W. Rabalais, Chem. Phys. Lett., 59 (1978) 356.
50. M.H. Rodriguez and H.E. Beske, Adv. in Mass Spectrom, 7A (1978) 593.
51. R.J. Day, S.E. Unger, and R.G. Cooks, JACS, 101 (1979) 499.
52. D.P. Leta, Ph.D. Thesis, Cornell University (1980).
53. D.P. Leta and G.H. Morrison, Anal. Chem., 52 (1980) 277.
54. G.H. Morrison and G. Slodzian, Anal. Chem., 47 (1975) 932A.
55. V.R. Deline, W. Katz, C.A. Evans, and P. Williams, Appl. Phys. Lett., 33 (1978) 832.
56. M.A. Rudat and G.H. Morrison, Surf. Sci., 82 (1979) 549.
57. G. Dearnaley, J.H. Freeman, and R.S. Nelson, Ion Implantation, American Elsevier Publ. Co. Inc., New York 1973, pp. 154-254.
58. G. Kiriakidis, J.S. Colligon, and S.P. Chenatin, Rad. Eff., 41 (1979) 119.
59. K. Seshan, Rad. Eff., 40 (1979) 29.
60. S.I. Romanov and L.S. Smirnov, Rad. Eff., 37 (1978) 121.
61. A. Lidow, J.F. Gibbons, V.R. Deline, and C.A. Evans, Appl. Phys. Lett., 32 (1978) 15.
62. A. Lidow, J.F. Gibbons, V.R. Deline, and C.A. Evans, Appl. Phys. Lett., 32 (1978) 572.

Table 1. Molecular-To-Implant Yield Ratios

<u>Molecular Ion</u>	<u>Implant: Matrix</u>	<u>MI[±]/I[±]</u>
GeP ⁻	Ge:InP	12
InTe ⁻	Te:InP	10
InTe ^{+a}	Te:InP	5
AsTe ⁺	Te:GaAs	5
GeAs ⁻	Ge:GaAs	Large ^b
SiP ⁻	Si:InP	4.8
GeP ⁻	P:Ge	2.8
SiP ⁻	Si:GaP	2.0
SiP ⁻	P:Si	0.9
SiAs ⁻	As:Si	0.8
SiF ⁺	F:Si	0.45
GeCl ⁺	Cl:Ge	0.13
GaTe ⁻	Te:GaP	0.1
SnAs ^{+a}	Sn:GaAs	0.08
SiBr ⁺	Br:Si	< 0.02
SiCl ⁺	Cl:Si	< 0.01
SiSb ⁻	Sb:Si	c
GeAs ⁻	As:Ge	d
GeP ⁻	Ge:GaP	e
InSe ⁻	Se:InP ^h	f
GaSe ⁻	Se:GaAs	f
GeBr ⁺	Br:Ge	f
GeSb ⁻	Sb:Ge	f
SiAs ⁻	Si:GaAs	g

- a Not a triple bond analogue
- b No Ge⁻ detected, (signal < 1cps)
- c Large SiSb⁻ signal, implant damage interferences of Sb⁻ signal
- d Large GeAs, As⁻ interference
- e Small GeP⁻ signal, no Ge⁻ detected (signal < 1cps)
- f Mass interference of both I[±] and MI⁻
- g Neither Si⁻ or SiAs detected (signal < 1cps)
- h See refs 61 and 62 for SIMS analyses of Se:GaAs

CAPTIONS

Figure 1 Depth profile of phosphorus implanted germanium showing the P⁻ implant (1) and the GeP⁻ molecular (2) maximum intensity of GeP⁻ is 3 times that of P⁻ peak.

Figure 2 Depth profile of ¹²¹Sb implanted silicon yielding the SiSb⁻ molecular (2). The Sb⁻ (1) peak intensity is 16 times greater than the SiSb⁻ signal but a gaussian distribution is not observed due to mass interference.

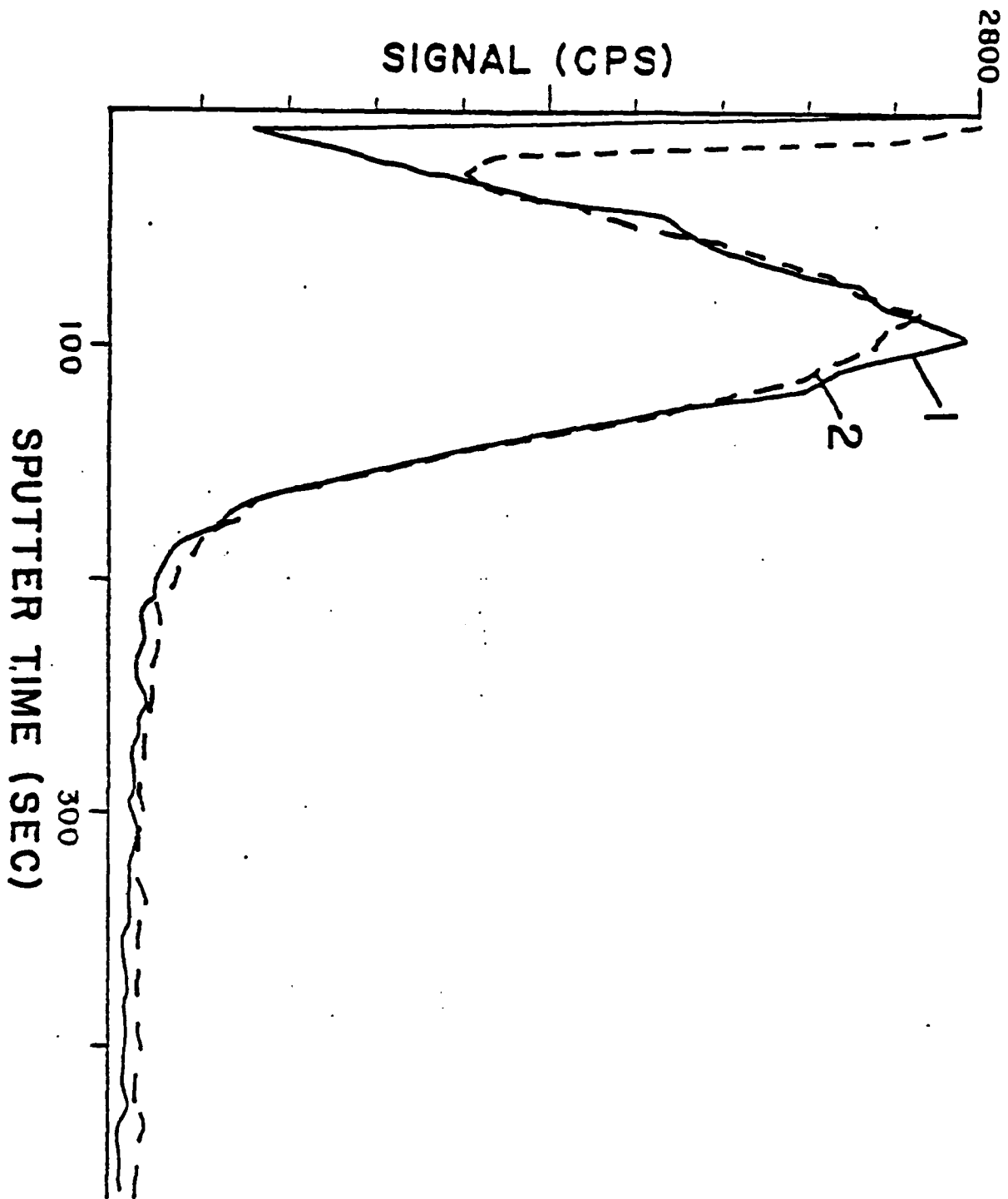


Figure 1.

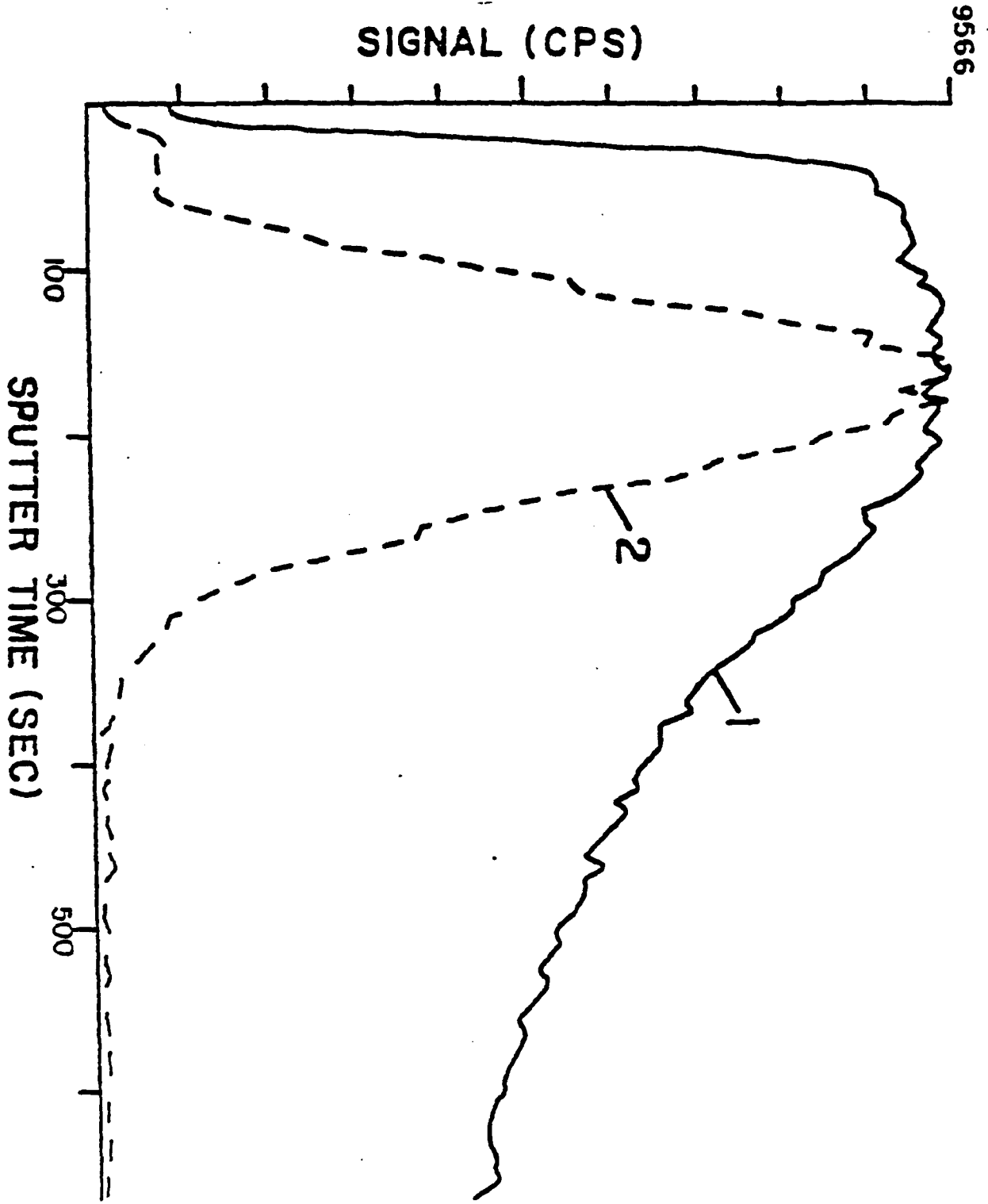


Figure 2.